CT Reconstruction of Surfaces from Binary Objects

S. Sawall[1,2], J. Kuntz[1], J. Maier[1], B. Flach[1,2], S. Schüller[1,2], and M. Kachelrieß[1,2]

[1]Medical Physics in Radiology, German Cancer Research Center (DKFZ), Heidelberg, Germany

[2]Institute of Medical Physics, Friedrich-Alexander-University (FAU), Erlangen, Germany

Purpose

Polygonal representations of objects obtained from computed tomography (CT) reconstructions are used in a variety of applications. Examples include finite element simulations (FEM) of biomechanical properties of bones or the assembly of antropomorphic phantoms [1]. The acquired rawdata are usually reconstructed onto a discrete voxel grid by an appropriate image reconstruction algorithm. In a subsequent step features of interest are segmented manually or by applying global and/or local thresholds, which are dependent on a variety of parameters. The obtained binary voxel objects are converted to polygonal meshes using appropriate algorithms, e.g. the marching cubes method, which again might be dependent on several parameters and are error-prone to miscalibrations of these variables. Such a pipeline is presented in figure 2. To overcome this issue we propose a reconstruction and refinement paradigm that operates on polygonal objects, i.e. meshes, and performs a modification of the mesh vertices such that the difference of a forward projection through this object and the acquired rawdata is minimized.

Materials and Methods

To estimate the shape of an object we restrict ourselves to meshes composed of triangles, as these are the most common primitives in the above mentioned applications. The shape of the object, i.e. its mesh, is found by optimizing the rawdata fidelity between a current estimate, given an initial guess, and the measured rawdata as show in figure 3 [2]. I.e. the triangle's vertices are deformed such that simulated intersections through the mesh match the acquired rawdata. This optimization requires the computation of a multitude of ray-triangle intersections to obtain the required intersection lengths. As a typical object might contain up to several million triangles, we employ a spatial subdivision structure, an octree, to allow for a rapid computation of intersection lengths through the considered meshes which also enables a highly performant incorporation of regularizations. This octree is a hierarchical, tree-like structure that sorts all triangles into spatially disjunct groups, each of them enclosed by a bounding box, which again contains eight smaller sub-boxes with corresponding sub-groups of triangles. The computation of the intersection length of a given ray through a mesh can be obtained by traversing the octree. Only triangles need to be considered for an intersection whose boxes are hit by the ray, reducing the number of ray-triangle intersection tests and highly improving performance. This approach is illustrated in figure 5 and the traversal of the octree in figure 6 [3].

Aim & Idea

- We aim at reconstructing object shapes, i.e. triangular meshes, based on acquired projection images.
- This allows for novel applications in engineering and medical sciences.
- The object shapes are obtained by optimizing the vertex positions of a given prior mesh to match the rawdata.
- As this optimization is performance critical we employ different optimization strategies, e.g. ordered subsets, and a spatial subdivision structure, an octree, to speed up computations.

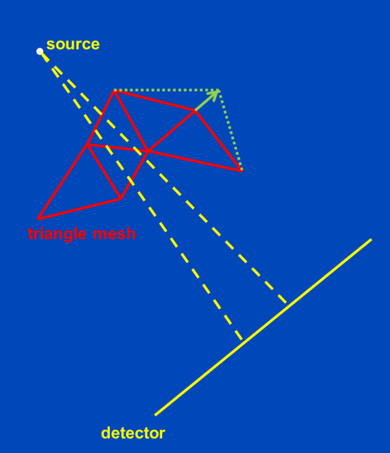

Figure 1: Basic methodology of the proposed method. The triangle mesh (red) is deformed to match the rawdata, resulting in a modified mesh (green).

Pipeline

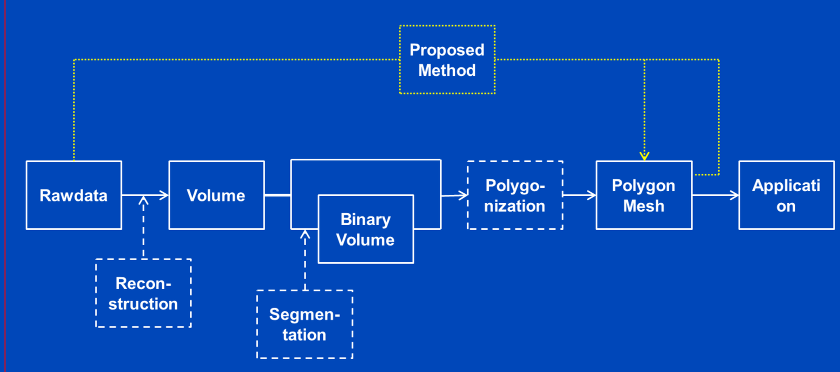

Figure 2: Schematic illustrating the proposed method (yellow) compared to the classic methodology containing several parameter dependent and error-prone steps.

Cost Function

We wish to optimize the following cost function given the measured rawdata p:

$$C(\mathbf{r}) = \|\mathbf{p} - \mu\mathbf{L}(\mathbf{r})\|_2^2 + \eta R(\mathbf{r}).$$

Therein, $r=(r_{x1}, r_{y1}, r_{z1}, \ldots, r_{zN})$ is the set of vertex coordinates to be optimized, L(r) is the intersection length of a ray through the mesh, μ the linear attenuation coefficient, and R(r) an optional regularization term.

The optimization is performed using a ordered subset accelerated gradient descent:

$$\mathbf{r}^{k+1} = \mathbf{r}^k + t\nabla_{\mathbf{r}} C(\mathbf{r}^k)$$

Figure 3: Proposed cost function, the variables used therein and a possible optimization scheme using a gradient descent.

Ray-Triangle Intersection

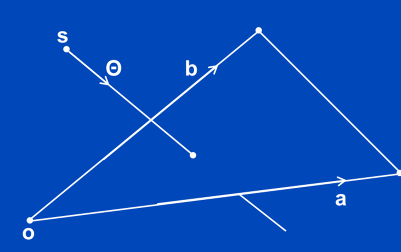

Given:

- a triangle with origin o and edges a and b

$$T(\mathbf{o}, \mathbf{a}, \mathbf{b}) = \{\mathbf{o} + \lambda_1\mathbf{a} + \lambda_2\mathbf{b}\}$$

- a ray originating at the source s in direction Θ

$$\mathbf{l}(\lambda) = \mathbf{s} + \lambda\boldsymbol{\Theta}$$

We find the intersection point with respect to s as:

$$\lambda = \frac{(\mathbf{a} \times \mathbf{b}) \cdot (\mathbf{o} - \mathbf{s})}{(\mathbf{a} \times \mathbf{b}) \cdot \boldsymbol{\Theta}}$$

Figure 4: Equations governing the computation of an intersection between a ray and a triangle.

Octree

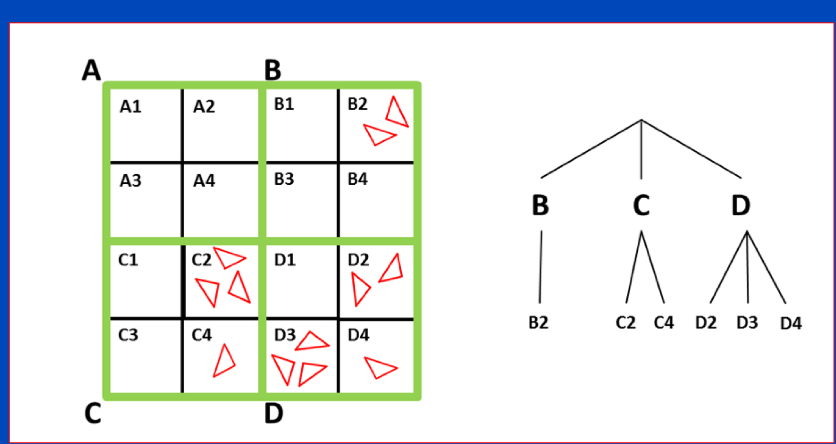

Figure 5: Sorting of triangles into bounding boxes (left) and the resulting octree structure (right) in case of two dimensions.

Octree Traversal

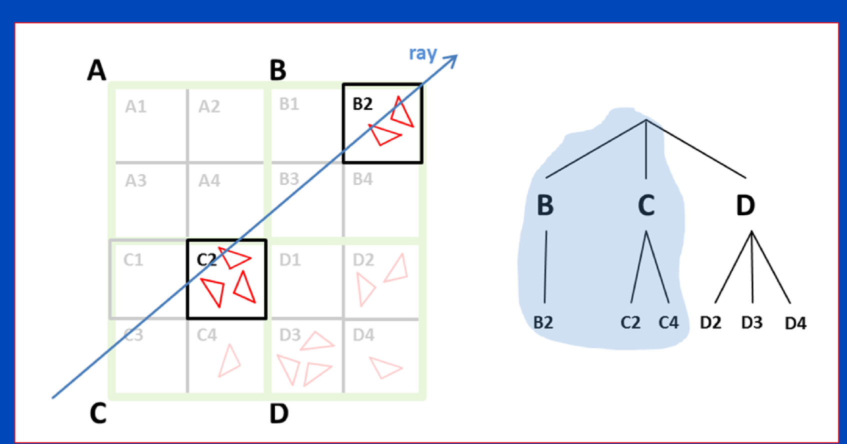

Figure 6: Traversal of the octree for a given ray only requires intersection tests with the highlighted triangles (left) and results in the consideration of only an octree branch (right).

Simulation Parameters

- Simulated scan:
  - Source-isocenter-distance: 572 mm
  - Isocenter-detector-distancer: 375 mm
  - Flat detector with 1000×1000 pixels each of 388 µm
  - 360 projections over 360°
- Simulated objects:
  - Human vertebra obtained from BodyParts3D (http://lifesciencedb.jp/bp3d/)
  - The vertebra contains 70000 triangles
  - The algorithm was initialized with a version of the vertebra that was scaled by a factor of 0.9 around its center of mass
- Test system:
  - 1 workstation with two Intel Xeon hexacore processor @ 3.46 GHz
  - 96 GB of RAM
  - Hyperthreading was disabled

Figure 7: Parameters used in the performed simulations as well as details on the used phantom and the test system.

Convergence

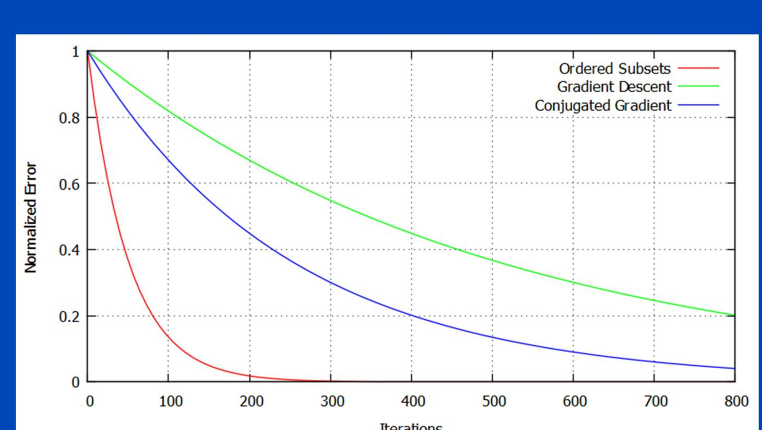

Figure 8: Convergence plot comparing the convergence speed of the different optimization strategies.

Results

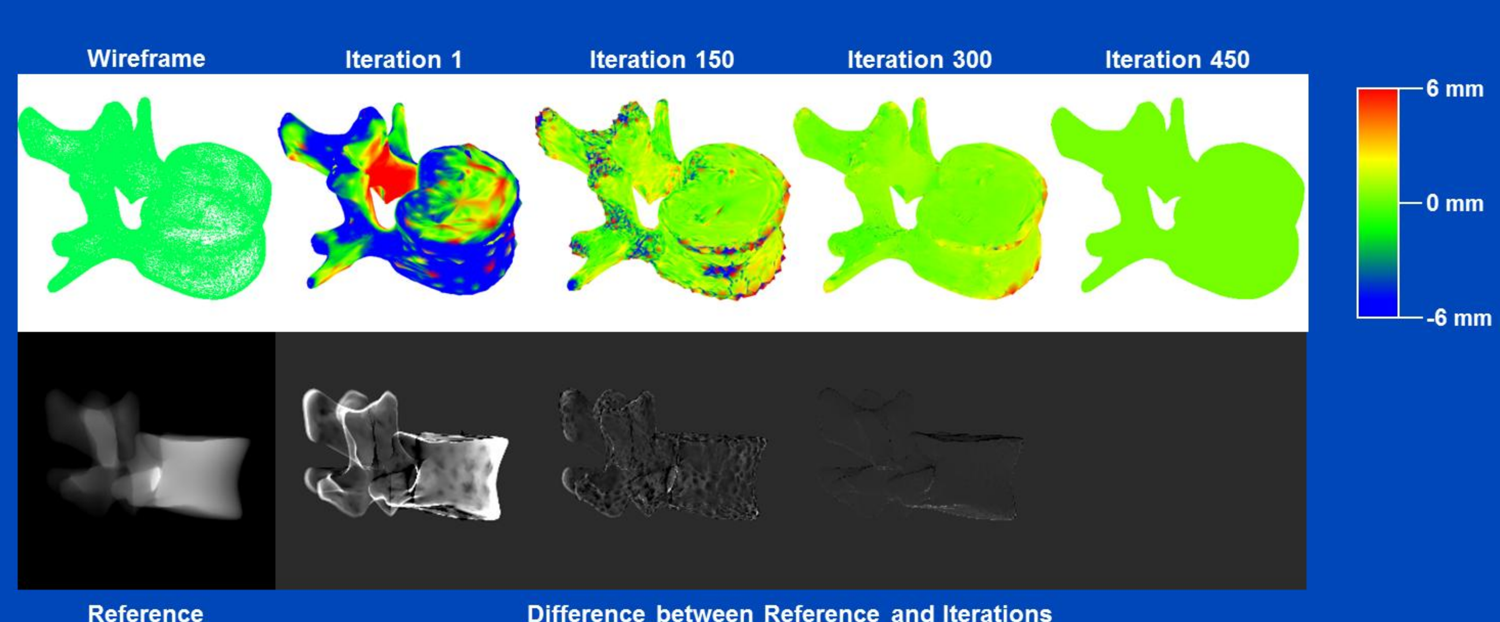

Figure 9: The top row shows colored deviation maps between the results obtained in a given iteration compared to the ground truth. The bottom row illustrates the difference projections between the estimates and the ground truth, showing that after 450 iterations the object was almost fully estimated and only negligible differences remain.

This ordering scheme further allows for a performant application of regularization strategies. In this study, however, we neglect the possibility of additional regularizations. The optimization of the cost function is performed using a gradient descent accelerated using ordered subsets and optional a conjugated gradient.

Results

To illustrate the capabilities of the proposed method, projections of a human vertebra [4] were simulated and a scaled version of this object was used as initial estimate. Further details on the simulations can be found in figure 7. Figure 8 compares the convergence speed of the above mentioned optimization strategies. The graph illustrates that an ordered subset accelerated gradient descent provides a much faster convergence speed than an optimization using a conjugated gradient. Figure 9 shows color coded deviation maps illustrating the differences between an estimate obtained in a given iteration compared to the ground truth. Note that distances are not computed between corresponding triangles in both models but between the surfaces closest to each other and thus the color coded deviation maps are not entirely blue but also reddish colors appear. In iteration 1 severe differences in the order of up to 6 mm exist. These errors are consequently reduced in the following iterations. After about 150 iterations only differences near edges remain which mostly vanished after 300 iterations. The estimated mesh corresponds to the ground truth after 450 iterations. This is further illustrated by the differences of projection images between ground truth and estimates shown in the bottom row of figure 9.

Conclusion

This feasibility study illustrates that the proposed method is capable of reconstructing triangle meshes from a given set of rawdata. As this task can be achieved in reasonable time in the scale of minutes it is a promising perspective to obtain detailed meshes from CT scans without the flaws of the usual methodology. Future research might include an estimation of the number of required projection images, the processing of multi-material objects and the integration of the proposed method into novel scan protocols.

References

[1] W. Segars, D. Lalush, and B. M. W. Tsui, “A realistic spline-based dynamic heart phantom,” *Nuclear Science, IEEE Transactions on*, vol. 46, no. 3, pp. 503-506, 1999.

[2] C. Soussen and A. Mohammad-Djafari, “Polygonal and polyhedral contour reconstruction in computed tomography,” *Image Processing, IEEE Transactions on*, vol. 13, no. 11, pp. 1507-1523, 2004.

[3] S. Sawall, M. Baer, M. Brehm, M. Knaup, and M. Kachelrieß, “Fast computation of projections from triangulated surfaces,” in *Fully 3D Image Reconstruction, 12th International Meeting on*, 2013, pp. 304-308.

[4] BodyParts3D. http://lifesciencedb.jp/bp3d/

Send correspondence request to:

Dr. Stefan Sawall
stefan.sawall@dkfz.de
German Cancer Research Center (DKFZ)
Im Neuenheimer Feld 280
69120 Heidelberg, Germany

dkfz.

CT Meeting 2014